Effects of low molecular weight organic acids on adsorption of Cd(II) by Auricularia auricula spent substrate-derived biochar: Types and reaction sequence

Xuesheng Liu, Yue Jiang, Wei Yang, Sha Li, Yu Jin, Juanjuan Qu, Wei Wang

PII: S2590-1826(24)00044-4

DOI: https://doi.org/10.1016/j.enceco.2024.09.001

Reference: ENCECO 150

To appear in: *Environmental Chemistry and Ecotoxicology*

Received date: 9 May 2024

Revised date: 29 July 2024

Accepted date: 27 September 2024

Please cite this article as: X. Liu, Y. Jiang, W. Yang, et al., Effects of low molecular weight organic acids on adsorption of Cd(II) by Auricularia auricula spent substrate-derived biochar: Types and reaction sequence, *Environmental Chemistry and Ecotoxicology* (2024), https://doi.org/10.1016/j.enceco.2024.09.001

Effects of low molecular weight organic acids on adsorption of Cd(II) by *Auricularia auricula* spent substrate-derived biochar：Types and reaction sequence

Xuesheng Liu[a], Yue Jiang[a], Wei Yang[a], Sha Li[a], Yu Jin[a], Juanjuan Qu[a,] *, Wei Wang[b,] *

[a] *College of Resources and Environmental Science, Northeast Agricultural University, Harbin, 150030, China*

[b] *Heilongjiang Academy of Black Soil Conservation and Utilization, Harbin, 150086, China*

*Corresponding author:

Juanjuan Qu (juanjuan4050234@163.com); Wei Wang (wangwei123873@163.com).

Abstract

Cadmium (Cd) is one of the most mobile and toxic heavy metals that seriously deteriorates crop quality and threatens human health. It is considered an effective means to stabilize Cd in soil and reduce plant uptake by the application of biochar. However, the interactions and mechanisms between biochar and Cd in the rhizospheric soil are blurred due to the involvement of low molecular weight organic acids (LMWOAs). In this study, four different reaction sequences were established to simulate the chemical interactions between LMWOAs and cadmium (Cd) in the rhizospheric soil with biochar. In terms of adsorption patterns, the results show that, LMWOAs not only slow down the adsorption of Cd ions onto biochar, but also desorb the adsorbed Cd ions from biochar. Tartaric acid (TA) makes adsorption easier, while citric acid (CA) and malic acid (MA) make it more difficult. In terms of adsorption mechanism, the functional groups of MA and CA on biochar the vary wtih reaction sequence, thereby affecting the Cd adsorption onto biochar. The functional groups of TA participate in the adsorption to the greatest extent, and its impact on adsorption is rarely influenced by the reaction sequence. The reaction sequence does not affect the types of Cd-crystals, but affects dissolvement or attachment to the surface of biochar. This study provides chemical insights for further understanding the impact of LMWOAs on the interaction between biochar and heavy metals in soil.

Keywords: Functional groups; Heavy metal; Rhizosphere; XRD; Mechanism

1. Introduction

Due to its high ecological toxicity, heavy metal pollution has become one of the most prevalent and severe issues (Liu et al., 2005; Luo et al., 2019). Heavy metal pollution reaches 82.8% of soil pollution in China, with cadmium (Cd) accounting for 7.0% (Pietrzak and Uren, 2011), posing serious threats to human health and ecosystems (Clemens et al., 2013). Biochar, known for its low cost and strong adsorption capacity, has attracted significant attention in soil remediation (Ali et al., 2020) (Huang et al., 2024; Li et al., 2021; Nkoh et al., 2022). In aqueous environments, functional groups on biochar surfaces can exchange ions with cadmium ions, where hydroxyl and carboxyl groups play key roles (Huang et al., 2024; Yu et al., 2024). In soils, beyond adsorption, biochar can alter soil properties (such as pH and cation exchange capacity), significantly impacting the speciation and mobility of cadmium (Liu et al., 2024; Song et al., 2024; Wang et al., 2024).

However, the interaction of biochar with Cd in soils is influenced by numerous factors, including soluble salt ions, pH, and low molecular weight organic acids (LMWOAs) (Islam et al., 2023; Islam et al., 2024; Rezwan et al., 2024; Zhao et al., 2024). LMWOAs in soil, such as oxalic acid (OA), tartaric acid (TA), formic acid (FA), citric acid (CA), acetic acid (AA), butyric acid (BA), lactic acid (LA), and malic acid (MA), primarily originate from root exudates, microbial metabolism, and the decomposition of plant and animal residues (Chen et al., 2013; Hinsinger et al., 2009; Qin et al., 2024; Taghipour and Jalali, 2013). In metal-contaminated soils, plants secrete more organic acids to adsorb and precipitate heavy metals, preventing their uptake by roots (Hseu et al., 2010; Renella et al., 2006; Sharma and Dietz, 2006; Sun et al., 2020), thereby reducing heavy metal absorption by plants (Agnello et al., 2014; Tao et al., 2019). Due to their diverse sources, the types and amounts of organic acids in soil are dynamically synthesized and decomposed (Jones, 1998). The concentration of rhizosphere organic acids generally ranges from 1 to 10 mmol/kg, or even higher, and is significantly higher in the rhizosphere soil compared to non-rhizosphere soil (Strobel, 2001). Therefore, the influence of LMWOAs in rhizosphere soils cannot be ignored.

Previous studies have shown that the leaching LMWOAs can enlarge the porosity and specific surface area of biochar by cleaning up the mineral blockages (Liu et al., 2017; Lou et al., 2011; Sun et al., 2016). LMWOAs can be physically adsorbed on the biochar surface

through electrostatic interactions of functional groups (Sun et al., 2016; Xie et al., 2015), or chemically adsorbed through esterification reactions between the -OH and -COOH groups in biochar and LMWOAs. Some LMWOAs, like CA, act as environmentally friendly chelating agents, effectively improving the accessibility of adsorption sites on the biochar surface (Nazari et al., 2019). LMWOAs can acidify biochar, altering its surface charge, which affects the adsorption and desorption of heavy metals (Hayakawa et al., 2018; Renella et al., 2004). Qiu's (2019) research showed that the adsorption capacity of biochar for Cd was enhanced after it was modified with CA, and the surface functional groups were the main contributor during Cd(II) adsorption. Additionally, organic anions can form stable complexes with heavy metal ions, leading to the transfer of heavy metals from the solid to the liquid phase (Nigam et al., 2001). Studies by Islam (2022a) showed that using low concentrations of CA (2 mmol/kg) and biochar can reduce the acid-soluble and bioavailable fractions of Cd in soil ($CaCl_2$-extractable), while higher concentrations of CA (>5-20 mmol/kg) had the opposite effect. Similar trends were observed with TA. All concentrations of OA increased the bioavailability of Cd (Islam et al., 2022b).

It can be seen that the effect of LMWOAs on the adsorption capacity of biochar is uncertain. It is reasonable to speculate that the reaction sequence of LMWOAs, biochar and Cd may affect the reaction results. However, the reaction sequence has not been paid attention to before. The interaction sequence of LMWOAs, biochar, and Cd has not been previously explored. This study focuses on the sequence of interactions because it affects the timing of biochar application. The dynamic changes in the content of low molecular weight organic acids in the rhizosphere soil, driven by plant root growth and activity, may lead to significant differences in Cd immobilization efficacy depending on the order of addition. Therefore, investigating how different sequences of adding biochar affect Cd adsorption is crucial for optimizing biochar use in the remediation of heavy metal-contaminated soils.

This study hypothesizes that the sequence of reactions involving LMWOAs, biochar, and Cd will influence the adsorption of Cd by biochar, and that the adsorption efficiency will vary depending on the type of LMWOAs used. To test this hypothesis, three different LMWOAs secreted by plants (TA, CA, MA) were selected for their distinct roles in soil chemistry: tartaric acid plays a crucial role in the soil by influencing nutrient availability and metal

mobility; citric acid enhances nutrient uptake by chelating minerals; and malic acid contributes to soil respiration and carbon cycling. The objectives were: (1) to study their effects on biochar's ability to immobilize Cd; and (2) to simulate different environmental conditions by varying the order of addition of Cd, biochar, and LMWOAs, and to explore changes in Cd immobilization efficiency. Specifically, the study was divided into the following four scenarios: (1) Cd, biochar, and LMWOAs are present simultaneously (simulating the application of biochar in Cd-contaminated soil with crop cultivation); (2) Cd reacts with LMWOAs first, followed by the addition of biochar (simulating crop cultivation in Cd-contaminated soil, followed by biochar application after some time); (3) Cd reacts with biochar first, followed by the addition of LMWOAs (simulating the addition of biochar to Cd-contaminated soil, followed by crop cultivation after some time); and (4) biochar reacts with LMWOAs first, followed by the addition of Cd (simulating biochar application in soil, followed by crop cultivation, and subsequent Cd contamination).

In conclusion, this study aims to explore the effects of reaction sequence on the interactions among LMWOAs, biochar, and Cd, elucidating the underlying mechanisms of these reactions. This will enhance our understanding of the interactions between biochar and heavy metals in the presence of rhizosphere exudates.

2. Material and methods

2.1 Biochar preparation, characterization, and physicochemical properties

The *Auricularia auricula* spent substrate used in this study was collected from the college of Resources and Environment, Northeast Agricultural University. After drying in an oven at 80 °C for 24 h, the *Auricularia auricula* spent substrate was heated under oxygen-limited environment at 400 °C for 2 h. This temperature was selected based on preliminary experiments, which indicated that biochar produced at 400 °C provided an optimal balance between yield and adsorption properties. After naturally cooling to room temperature, the black powder was smashed to pass through a 0.125 mm sieve prior, and the product was named biochar. The basic physical and chemical properties of biochar are shown in Table 1.

The X-ray diffraction (XRD) characterization was conducted to investigate the composition of minerals present in biochar sample with X-ray powder diffractometer (LEO 1455 VP/EDX Oxford 300, UK). The surface functional groups present in biochar were determined by

Fourier-transform infrared (FTIR) spectroscopy (Alpha, Bruker, Germany). Surface area was detected by N_2 adsorption isotherms at 77 K using an ASAP2460 surface area and porosity analyzer (Micromeritics, USA).

Biochar pH was determined in deionized water at a 1:20 (w: v) ratio. The biochar CEC was determined by the modified ammonium acetate compulsory displacement method, adapted to biochar (Domingues et al., 2017; Gaskin et al., 2008). The point of zero charge (pH_{pzc}) of biochar was achieved by a pH drift procedure (Suliman et al., 2016). Briefly, 0.05 g biochar was added to 25 mL of 0.01 mol·L^{-1} $CaCl_2$ solution pre-adjust to pH 2-12 using 0.1 mol·L^{-1} HCl or NaOH, and equilibrated for 24 h by continuous agitation in the dark before measurements. The pH_{pzc} value was obtained from the plateau parts of pH_{final} and $pH_{initial}$.

The acidic groups (carboxyl, lactone, and hydroxyl) covering the biochar surface were obtained by Boehm's titration method (Oickle et al., 2010). Briefly, 0.10 g of oven dried biochar samples were placed in 100 mL of each of three 0.05 mol·L^{-1} reaction bases: NaOH, Na_2CO_3, and $NaHCO_3$. The mixtures were agitated on an orbital shaker for 24 H and then filtered. After filtration, the unreacted alkaline solutions were titrated with 0.1 mol·L^{-1} standard HCl solution using methyl red as indicator, to ensure complete neutralization of bases. The contents of acidic groups were calculated under the assumption that NaOH neutralizes carboxylic, lactonic, and phenolic groups; Na_2CO_3 neutralizes carboxylic and lactonic groups; and $NaHCO_3$ neutralizes only carboxylic groups. The difference between molar $NaHCO_3$ and Na_2CO_3 was considered as the lactonic group surface concentration while the difference between molar NaOH and Na_2CO_3 was assumed to be the concentration of phenolic functional group (Mukherjee et al., 2011).

2.2 Batch experiment design

2.2.1 Adsorption of Cd(II) by biochar

The adsorption of Cd(II) onto biochar was determined using the batch method. In the batch experiment, 0.1 g of biochar particles were selected based on preliminary experiments to achieve high adsorption capacity with an economically rational dosage. A Cd(II) concentration of 30 mg·L^{-1} was chosen to represent environmentally relevant levels of contamination in soil systems. This concentration ensures measurable adsorption while avoiding excessive Cd concentrations that might alter adsorption dynamics. The background

solution consisted of 0.01 mol·L^{-1} NaCl to maintain ionic strength. To simulate acidic conditions favorable for Cd(II) adsorption onto biochar, the pH of the solution was adjusted to 5 using 1 mol·L^{-1} HCl or NaOH. The mixtures were shaken at 160 rpm and maintained at 25 °C for 24 hours to ensure equilibrium adsorption conditions. At the selected time intervals, the mixtures were sampled and filtered to separate the liquid solution and solid phase.

2.2.2 Adsorption of Cd(II) by biochar with the presence of LMWOAs

The Cd(II) adsorption experiments with LWMOAs were similar to that with individual biochar shown in the above section. Specifically, 5 mmol of three LMWOAs (TA, CA, and MA) and 1 g biochar was mixed in 1 L of 30 mg·L^{-1} Cd(II) solution. Basic informations of these selected LMWOAs are summarized in the Table 2. The solution of 30 mg·L^{-1} Cd(II) was prepared by dissolving an appropriate amount of $CdCl_2$ in 0.01 mol·L^{-1} NaCl background solution and the pH of the solution was adjusted to 5. Details of sampling and characterization method were similar to the adsorption experiment of Individual biochar. A series of control experiments including Cd(II) with LMWOAs but no biochar were set up following the same procedure above.

2.2.3 Effect of reaction sequence on the adsorption of Cd(II) by biochar

The influence of the reaction sequence among Cd(II) ions, biochar, and LMWOAs (5 mmol TA, CA or MA) on the adsorption of Cd(II) (30 mg·L^{-1}) onto biochar (1 g) was conducted in a series of 1L conical flask at pH 5.0 as following cases: (1) Cd, biochar and LMWOAs were added at the same time (denoted as BC+Cd+LMWOAs); (2) Cd and LMWOAs (5 mmol TA, CA, MA) were pre-equilibrated for 3 h before adding biochar [denoted as (Cd+LMWOAs)+BC]; (3)Cd and biochar were pre-equilibrated for 3 h before adding LMWOAs (5 mmol TA, CA, MA) [denoted as (Cd+BC)+LMWOAs]; (4) biochar and LMWOAs (5 mmol TA, CA, MA) were pre-equilibrated for 3 h before adding Cd [denoted as (BC+LMWOAs)+Cd]. Details of sampling and characterization method were similar to the adsorption experiment of biochar alone. The concentration of Cd(II) in the solution was measured by atomic absorption spectrophotometry (TAS-990).

The solutions were analyzed by atomic absorption spectrophotometry (TAS-990). The adsorption capacity was calculated using equations (1):

$$q_e = \frac{(C_0 - C_e)V}{m} \quad (1)$$

where C_0 (mg·L^{-1}) and C_e (mg· L^{-1}) represent the initial Cd(II) concentration and the Cd(II) concentration at the equilibrium, respectively, V represents the volume (mL) of the solution, and m represents the biochar mass (g).

2.3 Statistical analysis

All adsorption experiments were conducted in triplicate, and the averages were used in data analysis. Statistical analysis was performed using SPSS 24.0 and Origin 2022.

3 Results and discussion

3.1 Surface Morphology and Elemental Composition Analysis

Scanning electron microscopy (Figure 1) revealed that there are no significant morphological differences between the original biochar (BC) and the biochar treated with Cd and LMWOAs. All samples displayed similar grooves, pores, and fragments. EDX analysis (Tab. S1) indicates that the relative abundance of Cd on the biochar surface increased after Cd loading compared to the initial biochar. However, the abundance of Cd slightly decrease on the biochar surface after the involvement of LMWOAs. This result suggests that LMWOAs may have led to a decrease in the amount of Cd adsorbed on the biochar surface.

3.2 Effect of low-molecular-weight organic acids on Cd(II) adsorption

When LMWOAs, biochar, and Cd were simultaneously added (Figure 2a), the Q values of the three groups treated with LMWOAs were significantly lower than that of Cd+BC at 3 hours. After 6 hours, the Q values of the LMWOAs-treated groups increased substantially. By 24 hours, the Q values of all treatments were similar, reaching over 29 mg/g, indicating that nearly 100% of Cd ions were removed from the solution. This suggests that the addition of LMWOAs in the short term can inhibit the removal of Cd by biochar. However, LMWOAs can also react with Cd ions over a longer period untill capure all the ions.

When LMWOAs were added to the Cd solution first, followed by the addition of biochar (Figure 2b), the (Cd+TA)+BC group exhibited the highest Q value, and its Q value approached the maximum within 3 hours. The Q values of the (Cd+MA)+BC group were comparable to those of the Cd+BC group at all time points. The Q values of the (Cd+MA)+BC group were significantly lower than those of the other groups within 9 hours,

but approaching similar after 12 hours. This indicates that after Cd reacts with TA first, its reaction products are more easily removed from the solution by biochar.

In the case where biochar was added first followed by the addition of LMWOAs (Figure 2c), the Q values of all LMWOAs groups were significantly lower than those of the Cd+BC group. This indicates that all LMWOAs caused Cd desorption from the surface of biochar.

Under the condition where biochar reacted with LMWOAs first and then with Cd (Figure 2d), before 12 hours, the Q values ranked from high to low were (BC+TA)+Cd, BC+Cd, (BC+MA)+Cd, and (BC+CA)+Cd. However, by 24 hours, the Q values of all groups were close, indicating that Cd was essentially removed from the solution. The Q value of (BC+TA)+Cd approached the maximum at 3 hours. This results indicate that TA makes Cd removal more rapidly, while MA and CA makes Cd removal more difficult.

3.3 Solution pH and biochar cation exchange capacity (CEC)

The CEC values and pH values of the solutions after the reactions are illustrated in Figure 3. The CEC value of the BC+Cd group was the lowest at 15.56 cmol/g. All other groups exhibited significantly higher CEC values compared to the BC+Cd group, ranging from 29.76 to 53.10 cmol/g. Specifically, the average CEC for the BC+Cd+TA, BC+Cd+CA, and BC+Cd+MA groups was 31.52 cmol/g. For the (Cd+TA)+BC, (Cd+CA)+BC, and (Cd+MA)+BC groups, the average CEC was 30.79 cmol/g. The (Cd+BC)+TA, (Cd+BC)+CA, and (Cd+BC)+MA groups had an average CEC of 38.25 cmol/g, while the (BC+TA)+Cd, (BC+CA)+Cd, and (BC+MA)+Cd groups exhibited the highest CEC of 47.50 cmol/g. These values represent an increase of 157.71%, 241.26%, and 216.90%, respectively, compared to the BC+Cd group. This indicates that regardless of the addition sequence, LMWOAs alter the surface of biochar rather than solely reacting with Cd ions in the solution. Under the condition where LMWOAs first react with biochar, Cd ions are more likely to be adsorbed onto the surface of biochar in exchangeable forms. This could be attributed to the -COOH and -OH groups in LMWOAs occupying the adsorption sites on the surface of biochar, increasing the content of oxygen functional groups, and consequently enhancing the negative charge on the biochar surface, leading to an increase in CEC (Lonappan et al., 2020; Wang et al., 2022).

Comparing the final solution pH of each group (Figure 3), it is observed that the pH of all groups with added LMWOAs is lower than that of the BC+Cd group. This is attributed to the

alkaline nature of biochar (Table 1), while LMWOAs increase the concentration of hydrogen ions in the solution. Among all groups, the (Cd+BC)+TA, (Cd+BC)+CA, and (Cd+BC)+MA groups exhibited the lowest pH values. This indicates that LMWOAs participate in the reaction at a slower rate, and their addition maintains a higher concentration of hydrogen ions in the solution even after 24 hours. These hydrogen ions compete with Cd for the sites on the biochar surface, which is the reason why LMWOAs lead to a poor removal of Cd by biochar (Figure 2c).

In the pHpzc experiment (Figure 4), it was observed that the pHpzc values of all LMWOAs groups (ranging from 4.80 to 7.16) were lower than those of the BC+Cd group (pHpzc = 8.37). This indicates that the presence of LMWOAs (regardless of their addition sequence) can lower the pHpzc of biochar. Although the pHpzc values of (Cd+BC)+TA, (Cd+BC)+CA, and (Cd+BC)+MA were very low, the pH of the solutions after reaction (Figure 4) in each group was higher than their respective pHpzc values. This suggests that at the end of the reaction, the biochar surfaces in all groups carry negative charges, which is favorable for the adsorption of Cd ions. The difference in pHpzc values may be related to the difference in adsorption capacity of biochar for Cd ions, indicating that metal cations can be adsorbed and the negative charges can be neutralized on the biochar surface, or metal complexes can be formed.

3.4 Functional Groups and Compounds

The FTIR spectra (Figure 5) reveal that the spectral of biochar before and after reaction show relatively minor changes, with more peaks observed in the groups containing TA. All biochars exhibit an absorption peak at 3420 cm^{-1} attributed to -OH groups (Chen et al., 2014; Faheem et al., 2020), C-H bonds in aromatic groups appear near 3000 cm^{-1} (Huang et al., 2020), and -COOH stretching vibrations occur in the range of 1820-1648 cm^{-1} (Boehm, 2002; Novak et al., 2010). Other wavenumbers and corresponding functional groups are provided in Tables 3, 4, 5, and 6.

Comparing all peak positions (Tables S2, S3, S4, and S5), it is observed that after the reaction of biochar with Cd ions alone, notable changes in the wavenumbers representing -OH (1384), C-N (847), and C-H (584) are evident, indicating the involvement of these functional groups on the surface of biochar in the adsorption reaction. The groups BC+Cd+TA, BC+Cd+CA,

and BC+Cd+MA show additional peaks of some functional groups compared to the biochar group, such as C=O (1047-1049), indicating that these new functional groups have been loaded onto the surface of biochar. In comparison with the BC+Cd group, the representative wavenumbers of the C=O stretching peaks for BC+Cd+TA (1598) and BC+Cd+MA (1597), as well as the wavenumbers representing C-N peaks (882 and 888) for BC+Cd+TA and BC+Cd+MA, have changed. The R-O-C/R-O-CH3 peak wavenumbers (802 and 803) for the BC+Cd+CA and BC+Cd+MA groups have also changed.

After changing the addition sequence, some functional groups loaded onto biochar disappear, such as the C=O stretching peaks in the range of 1000-1200 for the (Cd+MA)+BC group, (Cd+BC)+MA group, (Cd+BC)+CA group, (Cd+CA)+BC group, and (Cd+MA)+BC group. This suggests that some functional groups in MA and CA may not ultimately be loaded onto the surface of biochar when the addition sequence has been changed, but may exist in a chelated form with Cd ions in the solution. However, in groups containing TA, regardless of its addition sequence, the highest number of functional groups retained in the range of 1000-1300 wavenumbers are observed, and based on the change in wavenumbers, it can be inferred that they all participate in the adsorption reaction.

The XRD spectra of biochar in each group are shown in Figure 6. In the BC+Cd group, the biochar surface is found to be coated with five types of Cd crystals (CdS, Cd6P7, Cd2P2S6, K2CdCl4, (CdZn)3P2), which is the highest among all groups. Although there are slight variations in diffraction peaks in other groups, no new Cd crystals are detected. In the groups with LMWOAs added, regardless of the addition sequence, the number of Cd crystal types in the groups containing TA is always higher than those containing CA and MA, Because in the TA-containing group, more Cd compounds are attached to the surface of biochar and easily form crystals after drying. Cd compounds in MA and CA groups may not be detected in the solution due to the weak acid desorption, which is consistent with the results of Q values and functional group detection.

3.5 Interaction between low molecular organic acids, biochar and Cd

Organic acids affected the adsorption of Cd(II) onto biochar may include the following five categories: (1) the functioning groups such as carboxyl on the biochar provided more adsorption sites, promoting biochar adsorption of Cd(II); (2) organic acid adsorption onto

biochar could increase the surface negative charge, increasing the number of adsorption sites; (3) organic acid could reduce the pH in the solution and increase the content of acid radical anions that could compete Cd(II) on biochar adsorption sites, thus inhibiting biochar adsorption of Cd(II); (4) organic acids could fill into the pores of biochar, anf reduce its adsorption capacity for Cd(II); (5) organic acids in liquid phase complex with Cd(II), reducing Cd(II) adsorption.

In this study, the addition of three types of organic acids showed both similarities and differences in their abilities of removing Cd ions from solution. The similarity lies in the fact that they all slowed down the adsorption of Cd ions by biochar. Additionally, they all exhibited significant desorption abilities, evidenced by the universal decrease in adsorption at all time points (Figure 2c). On one hand, this can be attributed to the acidity of LMWOAs, as hydrogen ions compete with Cd for sites on biochar. On the other hand, the acid anions of LMWOAs themselves can also complex with Cd ions, and the resulting complexes may not all present on the surface of biochar. Those dispersed complexes in the solution may not initially precipitate as solids at low pH but may be filtered out. However, as time progresses, the alkalinity of biochar gradually becomes prominent, raising the pH and potentially causing Cd ions or complexes to precipitate, leading to an increase in Q values. Further evidence is that the endpoint pH of all treatment solutions falls within the range of 5.5 to 8, an environment conducive to the formation of various precipitates containing Cd (Deng et al., 2019; Gundersen and Steinnes; 2003; Tran et al., 2016).

The differences lie in their respective effects on Q values. Under conditions of sufficiently reaction, TA reacts fastest, resulting in an increase in Q values, followed by CA and then MA. This difference may be related to the number of functional groups and dissociation constants (see Table 2). TA has more hydroxyl and carboxyl groups compared to CA and MA. The lower pKa1 and pKa2 values for TA, CA, and MA indicate stronger dissociation abilities, with the acid anions reacting more rapidly with Cd ions. This is consistent with the differences in their adsorption performance.

In this study, different reaction sequences were employed to represent various reaction conditions in rhizosphere soil. As plant roots gradually grow, the concentration of LMWOAs in the soil slowly increases, making the scenario of simultaneous reaction of LMWOAs,

biochar, and Cd (Cd+BC+LMWOAs) virtually impossible. Applying biochar to the soil after plant growth ((Cd+LMWOAs)+BC) is also impractical as burying biochar deeply would damage the plant roots. The most typical reaction sequences would be (Cd+BC)+LMWOAs or (BC+LMWOAs)+Cd. The (Cd+BC)+LMWOAs group (Figure 2c) simulates the scenario of applying biochar to Cd-contaminated soil followed by planting crops. Based on the results of this study, considering only the chemical mechanism, it can be inferred that LMWOAs secreted by roots cause desorption of Cd adsorbed on the biochar surface. Secretion of organic acids is one way plants obtain metal nutrients from the rhizosphere. However, in terms of chemical mechanism, LMWOAs do not distinguish nutrient ions from toxic ions. It can be speculated that Cd ions adsorbed by biochar may be activated by LMWOAs and leave away from its surface. Subsequently, due to the complexity of the soil environment, the desorbed Cd may undergo transformation into different forms, such as exchangeable, carbonate-bound, iron-manganese oxide-bound , organic-bound, or residual form, etc. Therefore, it cannot be conclusively determined that plants absorb more Cd due to desorption. (BC+LMWOAs)+Cd (Figure 2d) reflects the change in the adsorption capacity of Cd ions by biochar surface modified with LMWOAs. In soil solution, the adsorption of Cd ions may be influenced by the modification of biochar surface by LMWOAs. Among the three acids, TA evidently promotes surface adsorption, while CA and MA inhibit it, which indicates that the interaction between organic acids and biochar is complex and even contradictory. Additionally, as mentioned earlier, besides the ion form, Cd in the soil exists in various other forms, and the effect of modified biochar on these forms of Cd is still unclear.

Simulating soil environments in solution has its limitations. Firstly, the pH of different types of soil varies greatly, such as the red soil in southern China and the black calcareous soil in the north. Even within the same soil, the pH values at different distances from the root surface are not consistent. The pKa values help determine the degree of ionization of acids at a given pH, which is crucial for understanding their speciation and potential for complexation with metals like Cd(II) in the soil environment. If the soil pH is lower than pKa1, the acid will mostly be in its protonated form (H_2A). If the soil pH is between pKa1 and pKa2, the acid will mostly be in its partially deprotonated form (HA^-). If the soil pH is higher than pKa2, the acid will mostly be in its fully deprotonated form (A^{2-}). The deprotonated forms (HA^- or A^{2-})

have more negative charges and are more likely to form stable complexes with Cd(II). This is the case in our study. However, in practical applications, the pH range of the soil solution is broader, and it may be the key factor determining the stability of the complexes.

4. Conclusion

In this study, the chemical reaction patterns of biochar adsorption for Cd in the presence of LMWOAs (TA, CA, and MA) were investigated. All three LMWOAs slowed down the adsorption of Cd ions onto biochar. The Q values were influenced by the order of LMWOAs addition. When Cd was already adsorbed onto biochar, LMWOAs facilitated the desorption of Cd in a short period. LMWOAs altered the adsorption characteristics of biochar, with TA making adsorption easier while CA and MA making it relatively difficult. Mechanistically, changing the order of LMWOAs, biochar, and Cd affected the attachment of some functional groups in MA and CA to the biochar surface, thus impacting the adsorption of Cd. Among the three LMWOAs, TA exhibited the highest variety of functional groups involved in the reaction and was less influenced by the reaction sequence. The reaction sequence had minimal impact on the crystalline substances formed by Cd, with differences lying in whether they dissolved and how many types were attached to the biochar surface.

Declaration of Generative AI and AI-assisted technologies in the writing process

Statement:

During the preparation of this work the author used ChatGPT from Chat.openai.com to paraphrase sentences to improve the language. After using this tool/service, the author reviewed and edited the content as needed and takes full responsibility for the content of the publication.

Funding

This work was supported by China Postdoctoral Science Foundation (2021M700742) and Heilongjiang Postdoctoral Fund (LBH-Z21109).

Competing Interests

The authors declare that they have no known competing financial interests or personal relationships that could have appeared to influence the work reported in this paper.

References

Agnello, A. C., Huguenot, D., Van Hullebusch, E. D., and Esposito, G., 2014. Enhanced phytoremediation: a review of low molecular weight organic acids and surfactants used as amendments. Critical Reviews in Environmental Science and Technology, 44(22), 2531-2576. https://doi.org/10.1080/10643389.2013.829764

Ali, U., Shaaban, M., Bashir, S., Fu, Q., Zhu, J., Islam, M. S., Hu, H., 2020. Effect of rice straw, biochar and calcite on maize plant and Ni bio-availability in acidic Ni contaminated soil. Journal of Environmental Management, 2020, 259: 109674. https://doi.org/10.1016/j.jenvman.2019.109674

Boehm, H. P., 2002. Surface oxides on carbon and their analysis: a critical assessment. Carbon, 40(2), 145-149. https://doi.org/10.1016/S0008-6223(01)00165-8

Chen, T., Zhang, Y., Wang, H., Lu, W., Zhou, Z., Zhang, Y., Ren, L., 2014. Influence of pyrolysis temperature on characteristics and heavy metal adsorptive performance of biochar derived from municipal sewage sludge. Bioresource Technology, 164, 47-54. http://dx.doi.org/10.1016/j.biortech.2014.04.048

Chen, Y. T., Wang, Y., Yeh, K. C., 2017. Role of root exudates in metal acquisition and tolerance. Current Opinion in Plant Biology, 39, 66-72. https://doi.org/10.1016/j.pbi.2017.06.004

Clemens, S., Aarts, M. G., Thomine, S., Verbruggen, N., 2013. Plant science: the key to preventing slow cadmium poisoning. Trends in Plant Science, 18(2), 92-99. https://doi.org/10.1016/j.tplants.2012.08.003

Deng, R., Huang, D., Wan, J., Xue, W., Lei, L., Wen, X., Li, B., 2019. Chloro-phosphate impregnated biochar prepared by co-precipitation for the lead, cadmium and copper synergic scavenging from aqueous solution. Bioresource Technology, 293, 122102. https://doi.org/10.1016/j.biortech.2019.122102

Domingues, R. R., Trugilho, P. F., Silva, C. A., Melo, I. C. N. D., Melo, L. C., Magriotis, Z. M., Sanchez-Monedero, M. A., 2017. Properties of biochar derived from wood and high-nutrient biomasses with the aim of agronomic and environmental benefits. PloS One, 12(5), e0176884. https://doi.org/10.1371/journal.pone.0176884

Faheem, Du, J., Bao, J., Hassan, M. A., Irshad, S., Talib, M. A., Zheng, H., 2020. Efficient capture of phosphate and cadmium using biochar with multifunctional amino and carboxylic

moieties: kinetics and mechanism. Water, Air, and Soil Pollution, 231, 1-16. https://doi.org/10.1007/s11270-019-4389-1

Gaskin, J. W., Steiner, C., Harris, K., Das, K. C., Bibens, B., 2008. Effect of low-temperature pyrolysis conditions on biochar for agricultural use. Transactions of the ASABE, 51(6), 2061-2069. https://doi.org/10.13031/2013.25409

Gundersen, P., Steinnes, E., 2003. Influence of pH and TOC concentration on Cu, Zn, Cd, and Al speciation in rivers. Water Research, 37(2), 307-318. https://doi.org/10.1016/S0043-1354(02)00284-1

Hayakawa, C., Fujii, K., Funakawa, S., Kosaki, T., 2018. Effects of sorption on biodegradation of low-molecular-weight organic acids in highly-weathered tropical soils. Geoderma, 324, 109-118. https://doi.org/10.1016/j.geoderma.2018.03.014

Hinsinger, P., Bengough, A.G., Vetterlein, D., Young, M., 2009. Rhizosphere: biophysics, biogeochemistry and ecological relevance. Plant and Soil 321, 117–152. https://doi.org/10.1007/s11104-008-9885-9

Hseu, Z. Y., Su, S. W., Lai, H. Y., Guo, H. Y., Chen, T. C., Chen, Z. S., 2010. Remediation techniques and heavy metal uptake by different rice varieties in metal-contaminated soils of Taiwan: new aspects for food safety regulation and sustainable agriculture. Soil Science and Plant Nutrition, 56(1), 31-52. https://doi.org/10.1111/j.1747-0765.2009.00442.x

Huang, F., Gao, L. Y., Wu, R. R., Wang, H., Xiao, R. B., 2020. Qualitative and quantitative characterization of adsorption mechanisms for Cd^{2+} by silicon-rich biochar. Science of the Total Environment, 731, 139163. https://doi.org/10.1016/j.cep.2022.109054

Huang, W. H., Chang, Y. J., Lee, D. J. 2024. Layered double hydroxide loaded pinecone biochar as adsorbent for heavy metals and phosphate ion removal from water. Bioresource Technology, 391, 129984. https://doi.org/10.1016/j.biortech.2023.129984

Huang, Y., Liu, T., Liu, J., Xiao, X., Wan, Y., An, H., Luo, X., Luo, S., 2024. Exceptional anti-toxic growth of water spinach in arsenic and cadmium co-contaminated soil remediated using biochar loaded with Bacillus aryabhattai. Journal of Hazardous Materials, 133966. https://doi.org/10.1016/j.jhazmat.2024.133966

Islam, M. S., Gao, R L, Gao, J. Y., Song, Z. T., Ali, U., Hu, H. Q., 2022a. Cadmium, lead, and zinc immobilization in soil using rice husk biochar in the presence of citric acid. International

Journal of Environmental Science and Technology, 2022, 19: 567-580. https://doi.org/10.1007/s13762-021-03185-6

Islam, M. S., Kashem, M. A., Moniruzzaman, M., Parvin, A., Das, S., Hu, H., 2023. Cadmium, lead, and zinc immobilization in the soil using a phosphate compound with citric acid present. Environmental Technology, 1-18. https://doi.org/10.1080/09593330.2023.2298668

Islam, M. S., Rezwan, F., Kashem, M. A., Moniruzzaman, M., Parvin, A., Das, S., Hu, H., 2024. Impact of a phosphate compound on plant metal uptake when low molecular weight organic acids are present in artificially contaminated soils. Environmental Advances, 15: 100468. https://doi.org/10.1016/j.envadv.2023.100468

Islam, M. S., Song, Z., Gao, R., Fu, Q., Hu, H., 2022b. Cadmium, lead, and zinc immobilization in soil by rice husk biochar in the presence of low molecular weight organic acids. Environmental Technology, 43(16): 2516-2529. https://doi.org/10.1080/09593330.2021.1883743

Jones, D. L., 1998. Organic acids in the rhizosphere–a critical review. Plant and Soil, 205, 25-44. https://doi.org/10.1023/A:1004356007312

Li, Y., Yu, H., Liu, L., Yu, H., 2021. Application of co-pyrolysis biochar for the adsorption and immobilization of heavy metals in contaminated environmental substrates. Journal of Hazardous Materials, 420, 126655. https://doi.org/10.1016/j.jhazmat.2021.126655

Liu, G., Chen, L., Jiang, Z., Zheng, H., Dai, Y., Luo, X., Wang, Z., 2017. Aging impacts of low molecular weight organic acids (LMWOAs) on furfural production residue-derived biochars: porosity, functional properties, and inorganic minerals. Science of the Total Environment, 607, 1428-1436. https://doi.org/10.1016/j.scitotenv.2017.07.046

Liu, L., Fan, S., Wang, Z., Hu, J., 2024. Chemical speciation distribution, desorption characteristics, and quantitative adsorption mechanisms of cadmium/lead ions adsorbed on biochars. Arabian Journal of Chemistry, 17(4), 105669. https://doi.org/10.1016/j.arabjc.2024.105669

Liu, W. H., Zhao, J. Z., Ouyang, Z. Y., Soderlund, L., Liu, G. H., 2005. Impacts of sewage irrigation on heavy metal distribution and contamination in Beijing, China. Environment International, 31(6), 805-812. https://doi.org/10.1016/j.envint.2005.05.042

Lonappan, L., Liu, Y., Rouissi, T., Brar, S. K., Surampalli, R. Y., 2020. Development of biochar-based green functional materials using organic acids for environmental applications. Journal of Cleaner Production, 244, 118841. https://doi.org/10.1016/j.jclepro.2019.118841

Lou, L., Luo, L., Wang, L., Cheng, G., Xu, X., Hou, J., Xun, B., Hu, B., Chen, Y., 2011. The influence of acid demineralization on surface characteristics of black carbon and its sorption for pentachlorophenol. Journal of Colloid and Interface Science, 361(1), 226-231. https://doi.org/10.1016/j.jcis.2011.05.015

Luo, Luo, J., Tao, Q., Jupa, R., Liu, Y., Wu, K., Song, Y., Li, J., Huang, Y., Zou, L., Liang, Y., Li, T., 2019. Role of vertical transmission of shoot endophytes in root-associated microbiome assembly and heavy metal hyperaccumulation in Sedum alfredii. Environmental Science and Technology, 53(12), 6954-6963. https://doi.org/10.1021/acs.est.9b01093

Mukherjee, A., Zimmerman, A. R., Harris, W., 2011. Surface chemistry variations among a series of laboratory-produced biochars. Geoderma, 163(3-4), 247-255. https://doi.org/10.1016/j.geoderma.2011.04.021

Nazari, S., Rahimi, G., Nezhad, A. K. J., 2019. Effectiveness of native and citric acid-enriched biochar of Chickpea straw in Cd and Pb sorption in an acidic soil. Journal of Environmental Chemical Engineering, 7(3), 103064. https://doi.org/10.1016/j.jece.2019.103064

Nigam, R., Srivastava, S., Prakash, S., Srivastava, M. M., 2001. Cadmium mobilisation and plant availability–the impact of organic acids commonly exuded from roots. Plant and Soil, 230(1), 107-113. https://doi.org/10.1023/A:1004865811529

Nkoh, J. N., Ajibade, F. O., Atakpa, E. O., Abdulaha-Al Baquy, M., Mia, S., Odii, E. C., Xu, R., 2022. Reduction of heavy metal uptake from polluted soils and associated health risks through biochar amendment: A critical synthesis. Journal of Hazardous Materials Advances, 6, 100086. https://doi.org/10.1016/j.hazadv.2022.100086

Novak, J. M., Busscher, W. J., Watts, D. W., Laird, D. A., Ahmedna, M. A., Niandou, M. A., 2010. Short-term CO2 mineralization after additions of biochar and switchgrass to a Typic Kandiudult. Geoderma, 154(3-4), 281-288. https://doi.org/10.1016/j.geoderma.2009.10.014

Oickle, A. M., Goertzen, S. L., Hopper, K. R., Abdalla, Y. O., Andreas, H. A., 2010. Standardization of the Boehm titration: Part II. Method of agitation, effect of filtering and

dilute titrant. Carbon, 48(12), 3313-3322. https://doi.org/10.1016/j.carbon.2010.05.004

Pietrzak, U., and Uren, N. C., 2011. Remedial options for copper-contaminated vineyard soils. Soil Research, 49(1), 44-55. https://doi.org/10.1071/SR09200

Qin, F., Shan, X. Q., Wei, B., 2004. Effects of low-molecular-weight organic acids and residence time on desorption of Cu, Cd, and Pb from soils. Chemosphere, 57(4), 253-263. https://doi.org/10.1016/j.chemosphere.2004.06.010

Qiu, Y., Zhang, Q., Li, M., Fan, Z., Sang, W., Xie, C., Niu, D., 2019. Adsorption of Cd (II) from aqueous solutions by modified biochars: comparison of modification methods. Water, Air, and Soil Pollution, 230: 1-11. https://doi.org/10.1007/s11270-019-4135-8

Renella, G., Egamberdiyeva, D., Landi, L., Mench, M., Nannipieri, P., 2006. Microbial activity and hydrolase activities during decomposition of root exudates released by an artificial root surface in Cd-contaminated soils. Soil Biology and Biochemistry, 38(4), 702-708. https://doi.org/10.1016/j.soilbio.2005.06.021

Renella, G., Landi, L., Nannipieri, P., 2004. Degradation of low molecular weight organic acids complexed with heavy metals in soil. Geoderma, 122(2-4), 311-315. https://doi.org/10.1016/j.geoderma.2004.01.018

Rezwan, F., Kashem, M. A., Hu, H., Islam, M. S., 2024. Mechanisms of Metal Immobilization in the Soil by a Phosphate Compound with Low Molecular Weight Organic Acids Present. Communications in Soil Science and Plant Analysis, 2024: 1-22. https://doi.org/10.1080/00103624.2024.2362224

Sharma, S. S., Dietz, K. J., 2006. The significance of amino acids and amino acid-derived molecules in plant responses and adaptation to heavy metal stress. Journal of Experimental Botany, 57(4), 711-726. https://doi.org/10.1093/jxb/erj073

Song, P., Liu, J., Ma, W., Gao, X., 2024. Remediation of cadmium-contaminated soil by biochar-loaded nano-zero-valent iron and its microbial community responses. Journal of Environmental Chemical Engineering, 12(2), 112311. https://doi.org/10.1016/j.jece.2024.112311

Strobel, B. W., 2001. Influence of vegetation on low-molecular-weight carboxylic acids in soil solution-a review. Geoderma, 99(3-4), 169-198. https://doi.org/10.1016/S0016-7061(00)00102-6

Suliman, W., Harsh, J. B., Abu-Lail, N. I., Fortuna, A. M., Dallmeyer, I., Garcia-Perez, M., 2016. Modification of biochar surface by air oxidation: Role of pyrolysis temperature. Biomass and Bioenergy, 85, 1-11. https://doi.org/10.1016/j.biombioe.2015.11.030

Sun, B., Lian, F., Bao, Q., Liu, Z., Song, Z., Zhu, L., 2016. Impact of low molecular weight organic acids (LMWOAs) on biochar micropores and sorption properties for sulfamethoxazole. Environmental Pollution, 214, 142-148. https://doi.org/10.1016/j.envpol.2016.04.017

Sun, L., Cao, X., Tan, C., Deng, Y., Cai, R., Peng, X., Bai, J., 2020. Analysis of the effect of cadmium stress on root exudates of Sedum plumbizincicola based on metabolomics. Ecotoxicology and Environmental Safety, 205, 111152. https://doi.org/10.1016/j.ecoenv.2020.111152

Taghipour, M., Jalali, M., 2013. Effect of low-molecular-weight organic acids on kinetics release and fractionation of phosphorus in some calcareous soils of western Iran. Environmental Monitoring and Assessment, 185, 5471-5482. https://doi.org/10.1007/s10661-012-2960-y

Tao, Q., Zhao, J., Li, J., Liu, Y., Luo, J., Yuan, S., Li, B., Li, Q., Xu, Q., Yu, X., Huang, H., Li, X., Wang, C., 2019. Unique root exudate tartaric acid enhanced cadmium mobilization and uptake in Cd-hyperaccumulator Sedum alfredii. Journal of Hazardous Materials, 383, 121177. https://doi.org/10.1016/j.jhazmat.2019.121177

Tran, H. N., You, S. J., Chao, H. P., 2016. Effect of pyrolysis temperatures and times on the adsorption of cadmium onto orange peel derived biochar. Waste Management and Research, 34(2), 129-138. https://doi.org/10.1177/0734242X15615698

Wang, Y., Wang, C., Xiong, J., Zhang, Q., Shang, J., 2022. Effects of low molecular weight organic acids on aggregation behavior of biochar colloids at acid and neutral conditions. Biochar, 4(1), 20. https://doi.org/10.1007/s42773-022-00142-5

Wang, Y., Wang, X., Bing, Z., Zhao, Q., Wang, K., Jiang, J., Jiang, M., Wang, Q., Xue, R., 2024. Remediation of Cd (II), Zn (II) and Pb (II) in contaminated soil by KMnO4 modified biochar: Stabilization efficiency and effects of freeze–thaw ageing. Chemical Engineering Journal, 150619. https://doi.org/10.1016/j.cej.2024.150619

Xie, T., Reddy, K. R., Wang, C., Yargicoglu, E., Spokas, K., 2015. Characteristics and

applications of biochar for environmental remediation: a review. Critical Reviews in Environmental Science and Technology, 45(9), 939-969. https://doi.org/10.1080/10643389.2014.924180

Yu, X., Wang, X., Sun, M., Liu, H., Liu, D., Dai, J., 2024. Cadmium immobilization in soil using phosphate modified biochar derived from wheat straw. Science of the Total Environment, 171614. https://doi.org/10.1016/j.scitotenv.2024.171614

Zeng, W., Lu, Y., Zhou, J., Zhang, J., Duan, Y., Dong, C., Wu, W., 2024. Simultaneous removal of Cd (II) and As (V) by ferrihydrite-biochar composite: Enhanced effects of As (V) on Cd (II) adsorption. Journal of Environmental Sciences, 139, 267-280. https://doi.org/10.1016/j.jes.2023.04.020

Zhao, Z., Chen, J., Gao, S., Lu, T., Farooq, U., Gang, S., Lv, M., Qi, Z., 2024. Low-molecular-weight aromatic acids mediated the adsorption of Cd^{2+} onto biochars: effects and mechanisms. Environmental Science and Pollution Research, 31(10), 1-14. https://doi.org/10.1007/s11356-024-32253-w

Table 1 Physicochemical properties of original biochar.

Yield （%）	S_{BET} ($m^2 \cdot g^{-1}$)	pH	pH_{pzc}	CEC ($cmol \cdot kg^{-1}$)	Oxygen-containing functional group($mmol \cdot g^{-1}$)			
					Carboxyl	Lactone group	Phenolic hydroxyl	Total acidic
43.32	2.49	9.37	8.37	15.65	0.535	1.155	0.155	3.24

Table 2 Low-molecular-weight organic-acids used in this study.

	Tartaric acid	Citric acid	Malic acid
Abbreviation	TA	CA	MA
Molecular formula	$C_4H_6O_6$	$C_6H_6O_7$	$C_4H_6O_5$
Structure	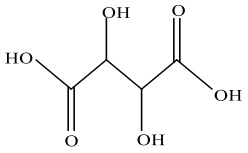	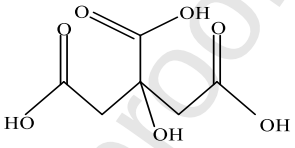	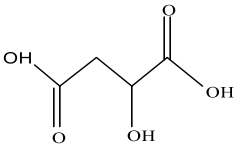
Carbon length	4	6	4
Molecular weight	150.09	192.13	134.09
Number of caboxylic groups	2	3	2
Number of hydroxy groups	2	1	1
Ligand form	H_2L	H_3L	H_2L
pK_{a1}	3.03	3.13	3.40
pK_{a2}	4.37	4.76	5.11
pK_{a3}	-	6.40	-

K_a for the dilute aqueous organic acid solution at 25 ℃.

Table 3 Physicochemical properties of biochar after adsorption.

	Oxygen-containing functional group ($mmol \cdot g^{-1}$)			
	Carboxyl	Lactone group	Phenolic hydroxyl	Total acidic
BC + Cd	0.48	1.045	1.445	2.97
BC + Cd + TA	1.475	0.785	1.95	4.21
BC + Cd + CA	0.165	1.625	1.49	3.28
BC + Cd + MA	0.42	1.05	1.01	2.48
(Cd + TA) + BC	2.375	0.71	1.535	4.62
(Cd + CA) + BC	0.3	1.575	1.735	3.61
(Cd + MA) + BC	0.515	1.425	1.64	3.58

(Cd + BC) + TA	1.45	1.185	2.305	4.94
(Cd + BC) + CA	0.875	1.635	2.37	4.88
(Cd + BC) + MA	0.95	1.26	2.18	4.39
(BC + TA) + Cd	2.455	0.105	2.48	5.04
(BC + CA) + Cd	0.935	0.795	1.25	2.98
(BC + MA) + Cd	0.915	0.04	0.775	1.73

Table S1 Relative abundance of elements (Wt%) on the biochar surface detected by EDX before and after adsorption.

Element	BC	BC+Cd	BC+Cd+TA	BC+Cd+CA	BC+Cd+MA
C	54.82	43.00	43.80	43.21	42.20
N	14.73	16.59	17.03	16.44	17.43
O	26.84	28.33	33.75	28.24	34.99
Na	0.42	0.28	1.02	0.44	0.92
Mg	0.46	0.45	0.19	0.45	0.23
Al	0.06	1.93	0.13	1.87	0.00
Si	0.11	5.29	0.64	5.29	0.50
Cd	0.64	1.37	1.00	1.25	1.07
K	0.96	1.20	0.97	1.33	0.58
Ca	0.96	1.57	1.48	1.52	2.08

Table S2 Peaks of each group of FTIR spectral lines and corresponding functional groups.

Wave number (cm^{-1})	BC	BC+Cd	BC+Cd+TA	BC+Cd+CA	BC+Cd+MA	Functional groups	Compounds
3200-3700	3416	3415	3412	3416	3405	OH stretching	acid, methanol
2700-3000	-	-	2961 2920 2849	2961 2920 2853	-	$C-H_n$ stretching	alkyl, aliphatic
1700-1730	-	-	-	-	-	C=O stretching	carboxyl, carbonyl
1450-1600	1586	1586	1598	1587	1597	C=O stretching	ketone and carbonyl
1420-1480	-	-	-	-	-	CH bending	aliphatic
1360-1430	1409	1384	1383	1382	1378	-OH, -CH bending O=C=O group $-CH_3$ deformation	hydrocarbon, acid, phenol, olefin and alcohol aryl-alkyl ether linkage, phenol, ketone, ether, phenol,
1200-	-	-	-	-	-	C-O stretching	chain

1300							anhydride
1000-1200	-	-	1047	1049	1047	C=O stretching	
						C-O-C stretching/bending	aromatic hydrogen
700-9000	873	847	882	876	888	C-N	
	780	779	779	802	803	R-O-C/R-O-CH_3	
400-700	593	584	610	598	594	C-H	
	469					C-C stretch or Mn-O, C-O-H bending, Fe-O stretch	

Table S3 Peaks of each group of FTIR spectral lines and corresponding functional groups.

Wave number (cm^{-1})	BC	BC+ Cd	(Cd+TA)+ BC	(Cd+CA)+ BC	(Cd+MA)+ BC	Functional groups	Compounds
3200-3700	3416	3415	3386	3415	3416	OH stretching	acid, methanol
2700-3000	-	-	-	2967	2916	$C-H_n$ stretching	alkyl, aliphatic
				2853	2922 2847		
1700-1730	-	-	-	-	-	C=O stretching	carboxyl, carbonyl
1450-1600	1586	1586	1591	1598	1598	C=O stretching	ketone and carbonyl
1420-1480	-	-	1438	-	-	CH bending	aliphatic
1360-1430	1409	1384	-	1378	1382	-OH, -CH bending	hydrocarbon, acid, phenol, olefin and alcohol
						O=C=O group	
						$-CH_3$ deformation	aryl-alkyl ether linkage, phenol, ketone, ether, phenol,
1200-1300	-	-	-	-	-	C-O stretching	chain anhydride
1000-1200	-	-	1130	1047	-	C=O stretching	
			1087			C-O-C stretching/ben	aromatic hydrogen

						ding	
700-9000	873	847 779	847	873	882	C-N	
	780	584	751	759	780	R-O-C/R-O-CH_3	
400-700	593		626	590	606	C-H	
	469					C-C stretch or Mn-O, C-O-H bending, Fe-O stretch	

Table S4 Peaks of each group of FTIR spectral lines and corresponding functional groups.

Wave number (cm^{-1})	BC	BC+Cd	(BC+Cd)+TA	(BC+Cd)+CA	(BC+Cd)+MA	Functional groups	Compounds
3200-3700	3416	3415	3387	3416	3416	OH stretching	acid, methanol
2700-3000	-	-	-	-	-	$C-H_n$ stretching	alkyl, aliphatic
1700-1730	-		-	-	-	C=O stretching	carboxyl, carbonyl
1450-1600	1586		1598	1598	1598	C=O stretching	ketone and carbonyl
1420-1480	-	-	1445	-	-	CH bending	aliphatic
1360-1430	1409	1586	1383	1378	1378	-OH, -CH bending	hydrocarbon, acid, phenol, olefin and alcohol
		-				O=C=O group	
		1384				$-CH_3$ deformation	aryl-alkyl ether linkage, phenol, ketone, ether, phenol,
1200-1300	-		-	-	1310	C-O stretching	chain anhydride
1000-1200	-		1135	-	-	C=O stretching	
		-	1087			C-O-C stretching/bending	aromatic hydrogen
700-9000	873	-	886	869	880	C-N	
	780	847	756	798	779	R-O-C/R-O-CH_3	

400-700	593	779	629	596	596	C-H	
	469	584		473	480	C-C stretch or Mn-O, C-O-H bending, Fe-O stretch	

Table S5 Peaks of each group of FTIR spectral lines and corresponding functional groups.

Wave number (cm^{-1})	BC	BC+ Cd	(Cd+TA)+ BC	(Cd+CA)+ BC	(Cd+MA)+ BC	Functional groups	Compounds
3200-3700	3416	3415	3387	3416	3416	OH stretching	acid, methanol
2700-3000	-	-	-	2961	-	$C-H_n$ stretching	alkyl, aliphatic
1700-1730	-		-	-	-	C=O stretching	carboxyl, carbonyl
1450-1600	1586		1590	1597	1598	C=O stretching	ketone and carbonyl
1420-1480	-	-	1440	-	-	CH bending	aliphatic
1360-1430	1409	1586	-	1379	1382	-OH, -CH bending	hydrocarbon, acid, phenol, olefin and alcohol
		- 1384				O=C=O group $-CH_3$ deformation	aryl-alkyl ether linkage, phenol, ketone, ether, phenol,
1200-1300	-		1294 1243	-	-	C-O stretching	chain anhydride
1000-1200	-	-	1129	-	-	C=O stretching	
		-	1087			C-O-C stretching/bending	aromatic hydrogen
700-9000	873	847	848	890	882	C-N	
	780	779	748	779	780	R-O-C/R-O-CH_3	
400-700	593	584	628	592	594	C-H	
	469				474	C-C stretch or Mn-O, C-O-H	

		bending, Fe-O stretch

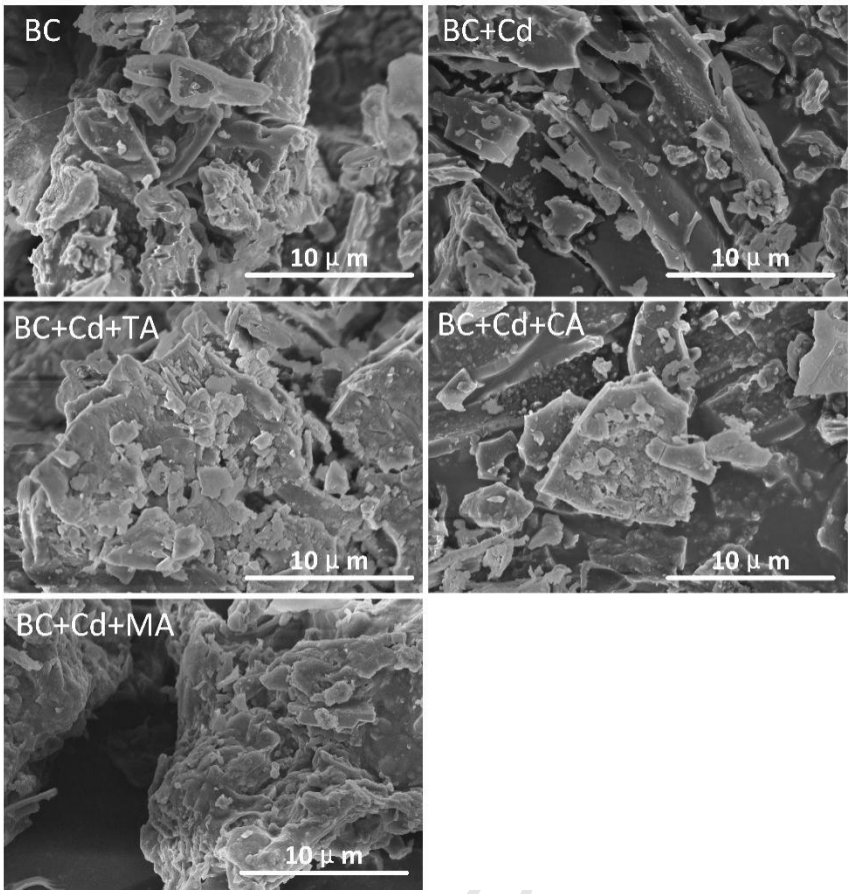

Figure 1 SEM images of initial biochar, Cd-loaded biochar, and biochar after adsorption reactions involving LMWOAs.

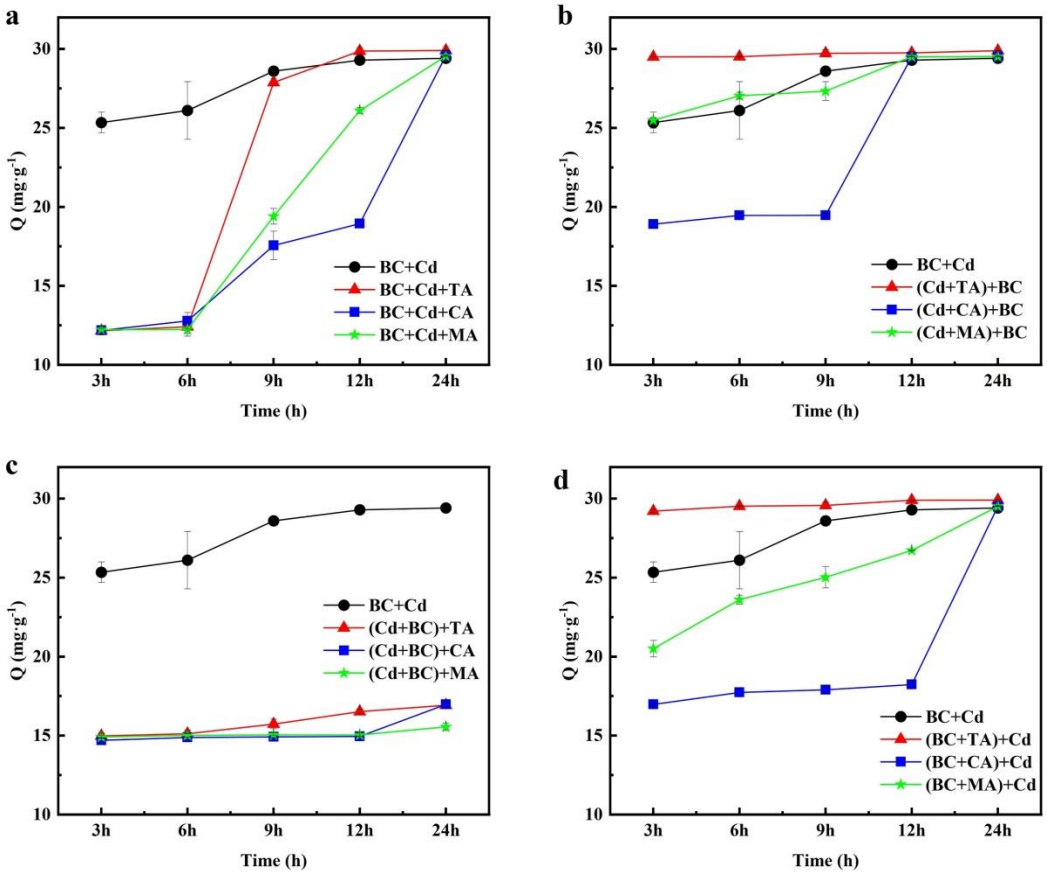

Figure 2. Q values of biochar adsorption of Cd ions under different reaction sequences.

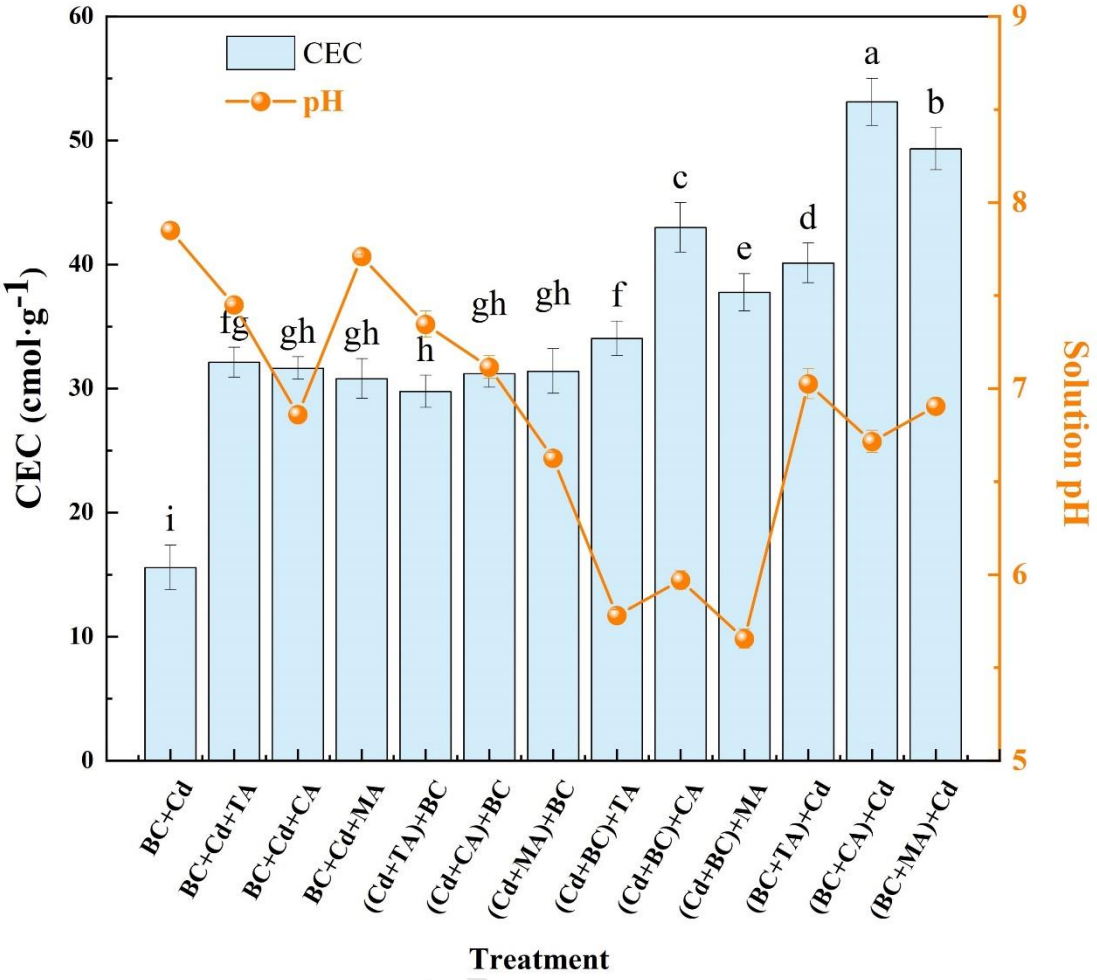

Figure 3 Influence of reaction sequence on the pH value and CEC (cation exchange capacity) of the solution at the reaction endpoint.

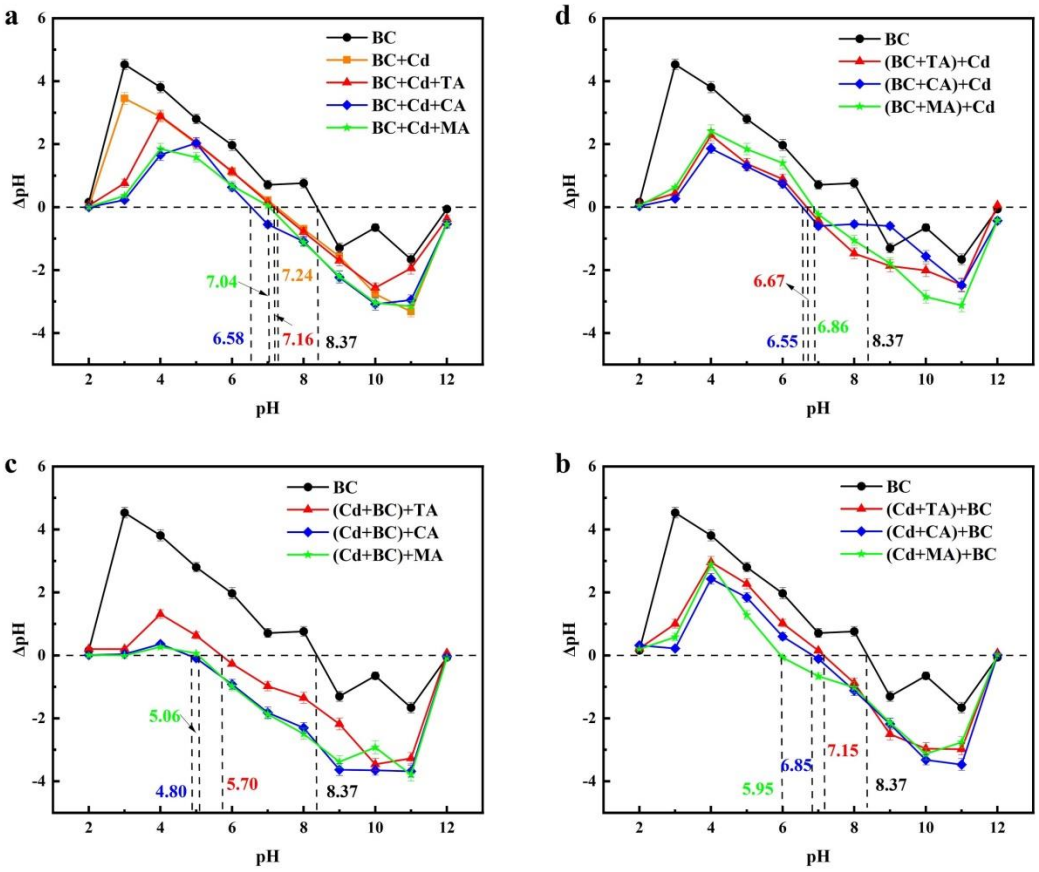

Figure 4 Point of zero charge (pHpzc) curves of each group.

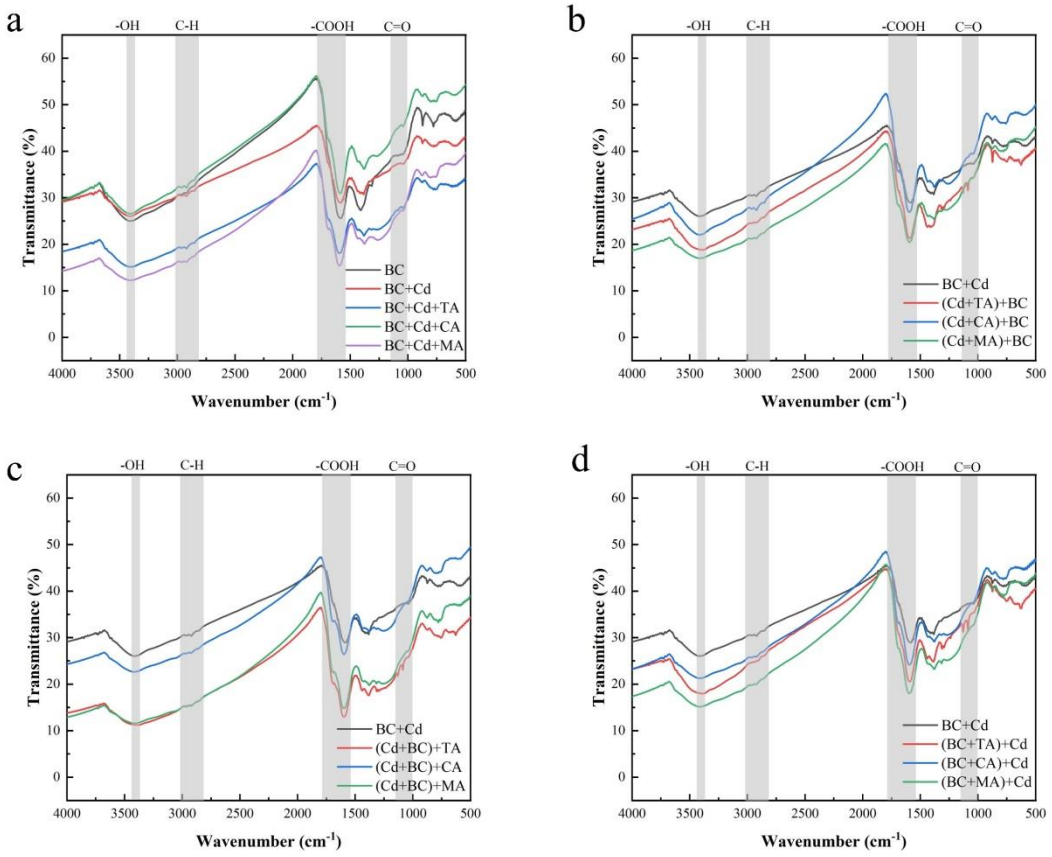

Figure 5 Comparison of FTIR spectral lines of biochar in each group.

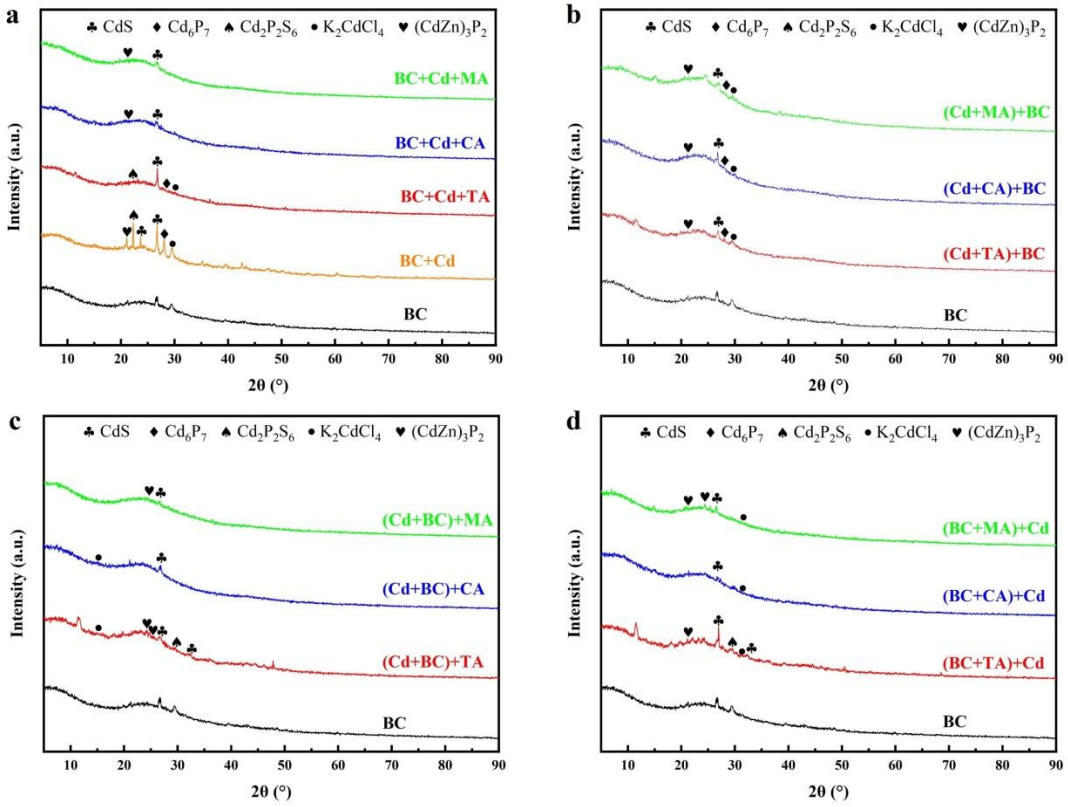

Figure 6 XRD patterns of each group of biochar after reaction.

Declaration of interests

☒ The authors declare that they have no known competing financial interests or personal relationships that could have appeared to influence the work reported in this paper.

☐The authors declare the following financial interests/personal relationships which may be considered as potential competing interests:

Highlights

Three LMWOAs slowed down the adsorption of Cd ions onto biochar.

The adsorption capacity of biochar varied with the reaction sequence.

The presence of LMWOAs facilitated the desorption of Cd from biochar.

Biochar loaded with TA possessed higher adsorption capacity for Cd.